Research Paper
Computational Methods for Differential Equations
http://cmde.tabrizu.ac.ir
Vol. 11, No. 4, 2023, pp. 834-850
DOI:10.22034/cmde.2023.53231.2245

A Legendre Tau method for numerical solution of multi-order fractional mathematical model for COVID-19 disease

Marjan Bidarian[1], **Habibollah Saeedi**[2,*], **and Mohammad Reza Balooch Shahryari**[1]

[1]Department of Mathematics, Kerman Branch, Islamic Azad University, Kerman, Iran.

[2]Department of Applied Mathematics, Faculty of Mathematics and Computer, Shahid Bahonar University of Kerman, Kerman, Iran.

Abstract

In this paper, we describe a spectral Tau approach for approximating the solutions of a system of multi-order fractional differential equations which resulted from coronavirus disease mathematical modeling (COVID-19). The non-singular fractional derivative with a Mittag-Leffler kernel serves as the foundation for the fractional derivatives. Also the operational matrix of fractional differentiation on the domain $[0, a]$ is presented. Then, the convergence analysis of the proposed approximate approach is established and the error bounds are determined in a weighted L^2 norm. Finally, by applying the Tau method, some of the important parameters in the model's impact on the dynamics of the disease are graphically displayed for various values of the non-integer order of the ABC-derivative.

Keywords. Multi-order fractional differential equation, Mathematical model of COVID-19, Fractional ABC-derivative, Mittag-Leffler kernel, Tau method, Error analysis.

2010 Mathematics Subject Classification. 34A08, 65L05, 65L20, 65L60.

1. Introduction

Mathematical models of infectious disease transmission dynamics play a significant role in supporting the quantification of possible infectious disease control and reduction strategies [15, 26–28, 31]. However, because each disease expresses its unique biological characteristics, different models have been introduced to each specific case to be able to confront real situations. Examples of these models include compartmental models, a SIR, SEIR, or other general-purpose model starting from the very traditional SIR model [1, 5, 6, 10, 16, 39].

In the past three years, an outbreak of a new infectious disease was reported which was caused by a novel coronavirus (SARS-CoV-2). Most persons who have COVID-19, as it is commonly known, will experience mild to moderate symptoms and recover without hospitalization. However, some people will get seriously sick and require medical care. So that by 28 November 2022, the number of infected cases confirmed by the World Health Organization (WHO) has reached about 650 million people worldwide while more than 6 million people of them have died. Eradicating this virus right now from the world is more like an impossible task. It's unrealistic. However, if the virus is not eradicated, then death, illness, or social isolation won't continue on the same scales as they have in the past. The future will depend heavily on the type of immunity people acquire through infection or vaccination and how the virus evolves. It would seem that the virus qualifies for endemic status already because of its global spread. But despite the fact that illnesses are spreading rapidly over the world and that a large number of people are still susceptible, scientists still consider the situation to be pandemic. Moreover, the coronavirus may be able to avoid immunity developed during infection and may even outsmart vaccines. Therefore, being knowledgeable about the condition and how the virus spreads is the greatest strategy to stop or slow down transmission. For this purpose, as was already indicated, one of

Received: 30 August 2022 ; Accepted: 10 April 2023.
∗ Corresponding author. Email: saeedi@uk.ac.ir.

the finest approaches to improve our comprehension of the situation is the mathematical modeling of the disease. This will make us further equipped to handle the situation and suggest effective strategies to stop the disease's spread.

Due to the COVID-19 pandemic's rapid spread, numerous beneficial studies on the mathematical modeling and analysis of this illness have been organized in a short period of time [1, 3, 22, 38]. These mathematical models try to describe the dynamics of COVID-19's evolutionary development so that can be used to predict the future behavior of its spread and make decisions to control it. COVID-19 is a communicable disease. According to the epidemiological data and recognized characteristics of the COVID-19 pandemic, we know that an exposed individual may interact with and transmit the virus to a susceptible individual. An interaction between the exposed individual and the susceptible individual may result in the susceptible individual becoming exposed. An exposed individual may experience an incubation period before becoming ill. Thus, an exposed person is infectious but not yet infected. An infected individual may be lucky enough to recover, at least to some extent, after some time. Alternatively, they will die. Hence, infectious diseases are dependent not only on the time instant but also on the previous time history. This process can be described by a dynamical system of differential equations. For this purpose, in preliminary research, the presented models were based on classical derivatives with some restrictions on the order of differential equations involved [25, 36, 38].

On the other hand, the fractional derivatives are not local operators, they proved to be accurate to describe processes with memory, i.e., calculating time-fractional derivative at point time requires the previous time, as is the case of many biological systems just like the COVID-19 disease. Moreover, the fractional differential equation is a possible tool to reduce the errors arising from the neglected parameters in the usual modeling of real-life phenomena. Fractional derivatives include essential features of cell rheological behavior and have enjoyed the greatest success in the field of rheology. Additionally, models in HIV made it clear that fractional models are more approximate than their integer order form [7, 13, 28, 29]. Therefore, several researchers try to apply fractional calculus instead derivatives with integer order[1, 3, 22, 23]. This led to the modeling of the COVID-19 disease using fractional differential equations (FDEs).

Numerous significant mathematical models are used in science, engineering, biology, chemistry, control theory, psychology, and medicine use fractional differential equations [1, 12, 30, 32, 34]. Due consideration should be given to the realistic modeling of physical phenomena that depend not only at the time instant but also on past time history, and since differential operators in fractional calculus have memory properties, these types of derivatives can aid in the display of many natural phenomena and facts with non-local dynamics behavior.

There are many different definitions of the generalization of the notion of differentiation to fractional orders e.g. Riemann-Liouville, Grünwald-Letnikow, Caputo, Generalized Functions Approach and other approaches [12, 14, 30, 33] in which the defined operators for fractional derivatives often have a weakly singular kernel and are not local. This property caused some derivatives of the solutions of fractional differential equations to have a singularity at the origin [17, 18]. Moreover, the corresponding integrals are not fractional integrals. To overcome this problem, recently, introduced a new type of derivative that is called the Atangana-Baleanu fractional derivative in Caputo sense (ABC-derivative), which is based on the generalized Mittag-Leffler function. Because it makes advantage of the Mittag-Leffler function's property, this definition has a non-singular and non-local kernel that may be used to many models [2, 4, 8, 9] including the Covide-19 disease modeling [3, 22, 23].

Most fractional differential equations do not have exact solutions and so, approximate and numerical techniques must be applied. Recently, providing various numerical methods for solving differential equations with fractional order has been receiving more attention by many authors [12, 17, 18, 24, 30, 33, 35]. In the last decades, spectral methods have been widely used for the numerical solving of various equations, due to their spectral rate of convergence. This feature makes those spectral methods provide superior accuracy [11, 17, 21, 37].

Therefore, considering the great importance of the Covid-19 disease and also the modeling of this disease with fractional equations, it is necessary to solve these equations with a suitable method that can yield accurate solutions such as the spectral methods with the spectral rate of convergence. The motivation of this paper is to present an effective numerical procedure with improved accuracy based on the spectral Tau method for the system of fractional differential equations derived from modeling the COVID-19 disease, together with the convergence analysis of the proposed method. Therefore, the objective of this research is to use a system of fractional differential equations with various orders to mathematically model this disease. To define the fractional derivatives based on the generalized

Mittag-Leffler function, we use the ABC-derivative. Since this operator is more accurate and flexible, it can be utilized to confidently represent such real-case issues. Then, this system of equations is solved using the spectral Tau approach and applying the method's convergence analysis, we demonstrate that the obtained numerical solutions have a spectral rate of convergence. Therefore, this method provides the appropriate numerical solutions which can be used to analyze the epidemic outcomes.

This paper is organized as follows: The next section is devoted to some required preliminaries and basic definitions of fractional derivatives that are used in the sequel. In section 3, we formulated the model together with the description of the parameters defined in the model. An explanation of the numerical method for solving the obtained mathematical model is described in section 4 and a convergence analysis of the proposed scheme is established in section 5. Finally, in section 6, some of the results and discussions of numerical simulations and the efficiency of the proposed scheme are reported by performing a numerical example. The conclusion of the article is summarized in section 7.

2. Preliminaries

In this section, we review the essential definitions and properties that are required next.

- As mentioned in previous section, there are several definitions for derivatives of fractional order. Here, the most common definition of fractional integration, Riemann-Liouville integral of order $\alpha \in (0,1)$ is defined as:

$$ {}^{R}I_t^{\alpha} f(t) = \frac{1}{\Gamma(\alpha)} \int_0^t (t-s)^{\alpha-1} f(s) ds, \tag{2.1}$$

where $\Gamma(\alpha)$ is the well known Gamma function and $t \in \Omega = [0,a]$ for $a > 0$. So, Caputo fractional derivative operator of order α is:

$$ {}^{C}D_t^{\alpha} f(t) = {}^{R}I_t^{1-\alpha} f'(t).$$

Properties of the above operators can be found in [12, 30]. As one can see, the kernels of these definitions are singular. The fractional ABC-derivative, which is a new class of fractional derivatives with a non-singular and non-local kernel that can sometimes accurately explain the dynamics of non-local phenomena, is introduced to state one's own problem.

- The Atangana-Baleanu fractional derivative in Caputo sense is defined as the following [8, 9, 20]:

Definition 2.1. Let $f(t)$ be a differentiable function on Ω such that $f'(t) \in L^1(\Omega)$ and $\alpha \in [0,1]$. The fractional ABC-derivative of $f(t)$ is given as:

$$ {}^{\mathcal{ABC}}\mathcal{D}_t^{\alpha} f(t) = \frac{\Re(\alpha)}{1-\alpha} \int_0^t f'(s)\, \Xi_{\alpha}\Big[\frac{-\alpha}{1-\alpha}(t-s)^{-\alpha}\Big] ds, \tag{2.2}$$

where $\Re(\alpha)$ is a normalization function with the main proprieties of $\Re(0) = \Re(1) = 1$ and defined by:

$$\Re(\alpha) = 1 - \alpha + \frac{\alpha}{\Gamma(\alpha)}.$$

Definition 2.2. Mittag-Leffler function $\Xi_{\alpha}(.)$ is defined as:

$$\Xi_{\alpha}(t) = \sum_{k=0}^{\infty} \frac{t^k}{\Gamma(k\alpha + 1)}.$$

From the definition of ABC-derivative, it is clear that it benefits Mittag-Leffler memory. Mittag-Leffler function has been recognized as one of the most important mathematical functions in fractional calculus and has many applications in various fields [2, 9, 20].

- The Atangana-Baleanu fractional integral operator of order α corresponding to ABC-derivative is defined as follows:

$$ {}^{\mathcal{ABC}}\mathcal{I}_t^{\alpha} f(t) = \frac{1-\alpha}{\Re(\alpha)} f(t) + \frac{\alpha}{\Gamma(\alpha)\Re(\alpha)} \int_0^t f(s)(t-s)^{\alpha-1} ds. \tag{2.3} $$

- According to these definitions, some of the useful relations for such derivatives which are applied in this article are as: (for more details see [2, 8, 9, 20])

$$ \begin{aligned} &{}^{\mathcal{ABC}}\mathcal{I}_t^{\alpha}\, {}^{\mathcal{ABC}}\mathcal{D}_t^{\alpha} f(t) = f(t) - f(0), \\ &{}^{\mathcal{ABC}}\mathcal{D}_t^{\alpha} t^{\beta} = \tfrac{\Re(\alpha)}{1-\alpha}\ t^{\beta}\ \Xi_{\alpha,\beta}\Big[\tfrac{-\alpha}{1-\alpha} t^{\alpha}\Big], \qquad \beta > [\alpha], \end{aligned} \tag{2.4} $$

where:

$$ \Xi_{\alpha,\beta}\Big[\frac{-\alpha}{1-\alpha} t^{\alpha}\Big] = \Gamma(1+\beta) \sum_{k=0}^{\infty} \Big(\frac{-\alpha}{1-\alpha}\Big)^k \frac{t^{\alpha k}}{\Gamma(1+\alpha k+\beta)}\ . $$

Furthermore, we can have the following Lemma for ABC-derivative.

Lemma 2.3. *Let $\mathcal{T} = [1, t, t^2, t^3, ..., t^N]^T$ be a standard basis vector. Then, we have:*

$$ {}^{\mathcal{ABC}}\mathcal{D}_t^{\alpha} \mathcal{T} = \mathbf{H}_t^{\alpha}\ \mathcal{T}, $$

where $\mathbf{H}_t^{\alpha}$ is a diagonal matrix whose first row ($j = 0$) is zero and diagonal entries are:

$$ \left(\mathbf{H}_t^{\alpha}\right)_{j,j} = \frac{\Re(\alpha)\Gamma(j+1)}{1-\alpha} \sum_{k=0}^{\infty} \Big(\frac{-\alpha}{1-\alpha}\Big)^k \frac{t^{\alpha k}}{\Gamma(j+1+\alpha k)}, \qquad j = 1, 2, ... \tag{2.5} $$

Proof. Applying the definition of ABC-derivative of order α and the second relation of Eq. (2.4), we will have:

$$ \begin{aligned} {}^{\mathcal{ABC}}\mathcal{D}_t^{\alpha}\mathcal{T} &= \Big[{}^{\mathcal{ABC}}\mathcal{D}_t^{\alpha}\ 1, {}^{\mathcal{ABC}}\mathcal{D}_t^{\alpha}\ t, \cdots, {}^{\mathcal{ABC}}\mathcal{D}_t^{\alpha}\ t^N\Big]^T \\ &= \left[0, \frac{\Re(\alpha)\Gamma(2)}{1-\alpha} \sum_{k=0}^{\infty} \Big(\frac{-\alpha}{1-\alpha}\Big)^k \frac{t^{\alpha k+1}}{\Gamma(2+\alpha k)}, \cdots, \frac{\Re(\alpha)\Gamma(N+1)}{1-\alpha} \sum_{k=0}^{\infty} \Big(\frac{-\alpha}{1-\alpha}\Big)^k \frac{t^{\alpha k+N}}{\Gamma(N+1+\alpha k)}\right]^T \\ &= \begin{bmatrix} 0 & 0 & 0 & \dots \\ 0 & \frac{\Re(\alpha)\Gamma(2)}{1-\alpha} \sum_{k=0}^{\infty} \Big(\frac{-\alpha}{1-\alpha}\Big)^k \frac{t^{\alpha k}}{\Gamma(2+\alpha k)} & 0 & \dots \\ \vdots & \vdots & \vdots & \ddots \end{bmatrix} \mathcal{T} \\ &= \mathbf{H}_t^{\alpha}\ \mathcal{T}, \end{aligned} $$

where $\mathbf{H}_t^{\alpha}$ is a diagonal matrix denoted in Eq. (2.5). □

Also, we need to recall some useful definitions and lemmas for norms that will be used in the sequel. These concepts can be found in references [11, 37].

- The space $L^2_{\widetilde{\alpha},\widetilde{\beta}}(\Omega)$ is the space of all functions $\vartheta(t)$ over Ω with respect to the Jacobi weight function $\omega^{\widetilde{\alpha},\widetilde{\beta}}(t) = \left(\frac{2}{a}\right)^{\widetilde{\alpha}+\widetilde{\beta}}\ t^{\widetilde{\alpha}}(a-t)^{\widetilde{\beta}}$ with parameters $\widetilde{\alpha}, \widetilde{\beta} > -1$ for which $\|\vartheta\|^2_{\widetilde{\alpha},\widetilde{\beta}} < \infty$. Therefore:

$$ \|\vartheta\|^2_{\widetilde{\alpha},\widetilde{\beta}} = \int_{\Omega} |\vartheta(t)|^2\ \omega^{\widetilde{\alpha},\widetilde{\beta}}\ dt. $$

In this paper, for simplicity, we apply the notation $(L^2(\Omega),\ \|.\|)$ when $\widetilde{\alpha} = \widetilde{\beta} = 0$.

- $\mathcal{S}^m(\Omega)$ is the non-uniform Sobolev space of all functions $\vartheta(t)$ over Ω which is defined by:

  $\mathcal{S}^m(\Omega) = \{\vartheta(t) \mid \|\vartheta\|_m < \infty\}$,

  associated with the following norm and semi-norm:

  $$\|\vartheta\|_m^2 = \sum_{k=0}^{m} \left\|\vartheta^{(k)}\right\|_{m,m}^2, \ |\vartheta|_m = \left\|\vartheta^{(m)}\right\|_{m,m}.$$

- Assume that the symbol $\langle .,. \rangle$ stands for the inner product defined by [21, 37]:

  $$\langle f, g \rangle = \int_{\Omega} f(t) g(t) \ dt, \tag{2.6}$$

  and $\langle .,. \rangle_N$ shows the discrete Legendre Gauss inner product defined by:

  $$\langle f, g \rangle_N \ = \sum_{j=0}^{N} f(t_j) \ g(t_j) \ \omega_j,$$

  where $\{t_j, \omega_j\}_{j=0}^{N}$ are the shifted Legendre Gauss nodal points and corresponding weights over Ω, respectively [21, 37].
- Let $\mathbb{P}_N$ be the space of all polynomials with a maximum degree of N on Ω and suppose that $\mathcal{L}_i(t) = J_i^{0,0}(\frac{2t-a}{a})$ denotes the shifted Legendre polynomials on $t \in \Omega$ so that $J_i^{0,0}$ is $i-$th Jacobi polynomial which is mutually orthogonal with respect to the uniform weight function $\omega(t) = 1$. Then, clearly:

  $\mathbb{P}_N = Span\{\mathcal{L}_0(t), \mathcal{L}_1(t), \cdots, \mathcal{L}_N(t)\}$,

  consequently, for any function $\vartheta(t) \in L^2(\Omega)$, we have the following unique expansion:

  $$\vartheta(t) = \sum_{i=0}^{\infty} \vartheta_i \ \mathcal{L}_i(t), \ \vartheta_i = \frac{\langle \vartheta, \mathcal{L}_i \rangle}{\|\mathcal{L}_i\|^2},$$

  and the orthogonal projection $\mathcal{P}_N(\vartheta(t)) : L^2(\Omega) \to \mathbb{P}_N$ is defined by:

  $$\mathcal{P}_N(\vartheta(t)) = \sum_{i=0}^{N} \vartheta_i \ \mathcal{L}_i(t),$$

  which has the following property:

  $\langle \mathcal{P}_N(\vartheta) - \vartheta, \ \psi \rangle = 0, \ \forall \ \psi \in \mathbb{P}_N.$

  Lemma 2.4. *[18, 37] Suppose that $\vartheta(t) \in \mathcal{S}^m(\Omega)$ for some $m \in \mathbb{N}_0$. Then we have:*

  $\left\|\mathcal{P}_N(\vartheta) - \vartheta\right\| \leq C \ N^{-m} \ |\vartheta|_m,$

  Lemma 2.5. *[18, 30] The Riemann-Liouville fractional integral operator ${}^R I_t^{\alpha}$ is bounded on $L^2(\Omega)$. On the other hand, for any $\vartheta \in L^2(\Omega)$, we have:*

  $\left\| \ {}^R I_t^{\alpha}(\vartheta(t))\right\| \leq C \ \|\vartheta(t)\|.$

Now, these preliminary steps are applied to model COVID-19 disease in the following.

Table 1. Used notations and their meaning.

Parameter	Description
τ	Transfer rate of $\mathbb{S}$ to $\mathbb{Q}$
β	Contact rate between $\mathbb{S}$ and $\mathbb{E}$
δ	Mortality rate in $\mathbb{I}_s$
γ	transfer rate of $\mathbb{E}$ to $\mathbb{Q}$
η	transfer rate of $\mathbb{E}$ to $\mathbb{I}_s$
σ	transfer rate of $\mathbb{E}$ to $\mathbb{I}_a$
θ	transfer rate of $\mathbb{Q}$ to $\mathbb{I}_a$
ζ_1	Recovery rate of $\mathbb{I}_a$
ζ_2	Recovery rate of $\mathbb{I}_s$
Λ	Recruitment (natality) rate
μ	Natural mortality rate

3. Model Formulating

In December 2019, the new coronavirus was discovered for the first time in the world. Numerous researchers have attempted to quantitatively analyze this problem because of the rapid spread of this disease and how important it is [3, 6, 23, 25], as mentioned in previous sections.

Due to that virus spreads when a healthy person comes into a contact with the virus carried out by an infected person. Some approximate solutions of the time-fractional equations involving fractional integrals without singular kernels can be used to heed some light on the expected time development. The researchers have shown that fractional derivatives in fact are defined utilizing convolutions that contain ordinary derivatives as a special case. Besides, the geometry of fractional derivatives tells us about the accumulation of the whole function. In fact, fractional operators are nonlocal with a memory effect, unlike ordinary differential operators which are local in nature. The memory property allows more knowledge from the past to be added, which predicts and translates models more accurately. The global dynamics of the relevant problems, which contain the integer order derivative as a special case, are produced by further exploring dynamics problems under fractional derivatives rather than integer order derivatives. On the other hand, due to the increased degree of freedom, mathematical models constructed with the aid of fractional operators are frequently more accurate and dependable than the integer-order case. According to these facts, the fractional order models provide a better understanding and give more insights into the pandemic. Therefore, in this paper, we use one of these models [3] which is formulated with the impact of quarantine, isolation, and environmental effects on the transmission dynamics of coronavirus with the application of ABC-derivative.

Suppose that the total population of humans is denoted by $\aleph(t)$ at time t which is classified into seven categories: $\mathbb{S}(t)$ as susceptible individuals, $\mathbb{E}(t)$ as exposed individuals, $\mathbb{I}_a(t)$ as asymptotically infected individuals, $\mathbb{I}_s(t)$ as symptomatic infected individuals, $\mathbb{Q}(t)$ as quarantined individuals, and $\mathbb{R}(t)$ are individuals that have recovered or remove from disease. Based on these assumptions, the total population is $\aleph(t) = \mathbb{S}(t)+\mathbb{E}(t)+\mathbb{Q}(t)+\mathbb{I}_a(t)+\mathbb{I}_s(t)+\mathbb{R}(t)$. Due to that, we take a random community where the total population is divided into these seven sub-populations. Therefore, each of the sub-populations can be represented as a percentage of the total population.

Also, we will denote the natural human natality rate by Λ and the mortality rate by μ. The parameters β and τ represent the rates of susceptible individuals getting infected by enough contact with exposed individuals or just traveling to quarantined classes, respectively. The exposed individuals may first, with the rate γ, join the quarantined class or get infected without symptoms (asymptomatic) with the rate σ or be placed in a symptomatic infected class at the rate of η. Also, quarantined individuals may pass to the infected through a test with symptoms or without symptoms at the rates of υ and θ, respectively. The asymptomatic infected individuals may recover at the rate of ζ_1 and the symptomatic infected individuals at the rate of ζ_2. The biological explanation of these parameters is given in Table 1.

Now, the system of multi-order fractional differential equations governed by these assumptions can be described in ABC-derivative operator form for COVID-19 disease as follows:

$$\begin{cases} {}^{\mathcal{ABC}}\mathcal{D}_t^{\alpha_1}\mathbb{S}(t) = \Lambda - (\tau+\mu)\ \mathbb{S}(t) - \beta\ \mathbb{S}(t)\ \mathbb{E}(t), \\ {}^{\mathcal{ABC}}\mathcal{D}_t^{\alpha_2}\mathbb{E}(t) = \beta\ \mathbb{S}(t)\ \mathbb{E}(t) - (\gamma+\mu+\eta+\sigma)\ \mathbb{E}(t), \\ {}^{\mathcal{ABC}}\mathcal{D}_t^{\alpha_3}\mathbb{Q}(t) = \tau\ \mathbb{S}(t) + \gamma\ \mathbb{E}(t) - (\mu+\upsilon+\theta)\ \mathbb{Q}(t), \\ {}^{\mathcal{ABC}}\mathcal{D}_t^{\alpha_4}\mathbb{I}_a(t) = \sigma\ \mathbb{E}(t) + \theta\ \mathbb{Q}(t) - (\mu+\zeta_1)\ \mathbb{I}_a(t), \\ {}^{\mathcal{ABC}}\mathcal{D}_t^{\alpha_5}\mathbb{I}_s(t) = \eta\ \mathbb{E}(t) + \upsilon\ \mathbb{Q}(t) - (\mu+\delta+\zeta_2)\ \mathbb{I}_s(t), \\ {}^{\mathcal{ABC}}\mathcal{D}_t^{\alpha_6}\mathbb{R}(t) = \zeta_1\ \mathbb{I}_a(t) + \zeta_2\ \mathbb{I}_s(t) - \mu\ \mathbb{R}(t), \end{cases} \tag{3.1}$$

subject to the non-negative initial conditions:

$$\mathbb{S}(0)=\mathbb{S}_0, \quad \mathbb{E}(0)=\mathbb{E}_0, \quad \mathbb{Q}(0)=\mathbb{Q}_0, \quad \mathbb{I}_a(0)=\mathbb{I}_{a0}, \quad \mathbb{I}_s(0)=\mathbb{I}_{s0}, \quad \mathbb{R}(0)=\mathbb{R}_0.$$

The discussions of the existence and uniqueness of the solutions for the proposed model and stability analysis of the equilibrium points are explained in the reference [3]. For this purpose, they apply the basic reproduction number denoted by $\mathcal{R}_0$ which is the expected value of infection rate per time unit. This number defines as:

$$\mathcal{R}_0 = \frac{\beta\ \Lambda}{(\gamma+\mu+\eta+\sigma)(\tau+\mu)}.$$

In all cases, $\mathcal{R}_0 < 1$ implies that disease will decline, whereas $\mathcal{R}_0 > 1$ implies that disease will persist within a community and $\mathcal{R}_0 = 1$ requires further investigation. The following two theorems were addressed by authors in [3] in relation to stability:

Theorem 3.1. *The disease free equilibrium is globally asymptotically stable if* $\mathcal{R}_0 < 1$.

Theorem 3.2. *The endemic equilibrium is globally asymptotically stable.*

Thus, in this article, we focus on the solutions of these equations that can be useful to analyze the dynamic behavior and spread of the disease which can help to predict the future situation and even control of COVID-19 pandemic. Due to the fact that the system of fractional differential equations does not have an exact solution, in the following, we provide a numerical scheme for solving such equations.

4. Numerical Method

The main goal of this section is to demonstrate a spectral Tau method based on the shifted Legendre functions on Ω for approximating the numerical solutions of (3.1). In this case, we assume that the approximate solutions of (3.1) are given by:

$$\begin{cases} \mathbb{S}_N(t) \cong \sum_{i=0}^N s_i\mathcal{L}_i(t) = S\ \underline{L} = S\ L\ \mathcal{T}, \\ \mathbb{E}_N(t) \cong \sum_{i=0}^N e_i\mathcal{L}_i(t) = E\ \underline{L} = E\ L\ \mathcal{T}, \\ \mathbb{Q}_N(t) \cong \sum_{i=0}^N q_i\mathcal{L}_i(t) = Q\ \underline{L} = Q\ L\ \mathcal{T}, \\ \mathbb{I}_{aN}(t) \cong \sum_{i=0}^N a_i\mathcal{L}_i(t) = A\ \underline{L} = A\ L\ \mathcal{T}, \\ \mathbb{I}_{sN}(t) \cong \sum_{i=0}^N m_i\mathcal{L}_i(t) = M\ \underline{L} = M\ L\ \mathcal{T}, \\ \mathbb{R}_N(t) \cong \sum_{i=0}^N r_i\mathcal{L}_i(t) = R\ \underline{L} = R\ L\ \mathcal{T}, \end{cases} \tag{4.1}$$

where $\mathcal{T} = [1, t, t^2, ..., t^N]^T$ is the standard basis and:

$$\underline{L} = \left[\mathcal{L}_0(t), \mathcal{L}_1(t), ..., \mathcal{L}_N(t)\right]^T = L\ \mathcal{T},$$

in which L is a nonsingular lower triangular coefficient matrix of order $N+1$ given by:

$$L := \begin{pmatrix} 1 & & & & & \\ -1 & \frac{2}{a} & & & & \\ 1 & -\frac{6}{a} & \frac{6}{a^2} & & & \\ -1 & \frac{12}{a} & -\frac{30}{a^2} & \frac{20}{a^3} & & \\ 1 & -\frac{20}{a} & \frac{90}{a^2} & -\frac{140}{a^3} & \frac{70}{a^4} & \\ \vdots & \vdots & \vdots & \vdots & \vdots & \ddots \end{pmatrix}.$$

Also, $S = [s_0, s_1, ..., s_N]$, $E = [e_0, e_1, ..., e_N]$, $Q = [q_0, q_1, ..., q_N]$, $A = [a_0, a_1, ..., a_N]$, $M = [m_0, m_1, ..., m_N]$ and $R = [r_0, r_1, ..., r_N]$ are the unknown vectors. Substituting the approximate solutions (4.1) into (3.1) yields:

$$\begin{cases} S\ L\ {}^{\mathcal{ABC}}\mathcal{D}_t^{\alpha_1}(\mathcal{T}) = \Lambda\ I_{N+1} - (\tau+\mu)\ S\ L\ \mathcal{T} - \beta\ S\ L\ \Phi(E,L)\ \mathcal{T}, \\ E\ L\ {}^{\mathcal{ABC}}\mathcal{D}_t^{\alpha_2}(\mathcal{T}) = \beta\ S\ L\ \Phi(E,L)\ \mathcal{T} - (\gamma+\mu+\eta+\sigma)\ E\ L\ \mathcal{T}, \\ Q\ L\ {}^{\mathcal{ABC}}\mathcal{D}_t^{\alpha_3}(\mathcal{T}) = \tau\ S\ L\ \mathcal{T} + \gamma\ E\ L\ \mathcal{T} - (\mu+\upsilon+\theta)\ Q\ L\ \mathcal{T}, \\ A\ L\ {}^{\mathcal{ABC}}\mathcal{D}_t^{\alpha_4}(\mathcal{T}) = \sigma\ E\ L\ \mathcal{T} + \theta\ Q\ L\ \mathcal{T} - (\mu+\zeta_1)\ A\ L\ \mathcal{T}, \\ M\ L\ {}^{\mathcal{ABC}}\mathcal{D}_t^{\alpha_5}(\mathcal{T}) = \eta\ E\ L\ \mathcal{T} + \upsilon\ Q\ L\ \mathcal{T} - (\mu+\delta+\zeta_2)\ M\ L\ \mathcal{T}, \\ R\ L\ {}^{\mathcal{ABC}}\mathcal{D}_t^{\alpha_6}(\mathcal{T}) = \zeta_1\ A\ L\ \mathcal{T} + \zeta_2\ M\ L\ \mathcal{T} - \mu\ R\ L\ \mathcal{T}, \end{cases} \tag{4.2}$$

where I_{N+1} is the identity matrix of order $N+1$ and $\Phi(E,L)$ is an infinite upper triangular Toeplitz matrix [19] having the following structure:

$$\Phi(E,L) = \begin{bmatrix} E\ L_0 & E\ L_1 & E\ L_2 & \dots \\ 0 & E\ L_0 & E\ L_1 & \dots \\ 0 & 0 & E\ L_0 & \dots \\ \vdots & \vdots & \vdots & \ddots \end{bmatrix},$$

and $\{L_i\}_{i=0}^{\infty}$ is the $i-$th column of the coefficient matrix L. Here, we choose only the $N+1$ row and column of the Toeplitz matrix, in order to match its rank with the other matrices utilized in the system described above. By using Lemma 2.3 in (4.2), we have:

$$\begin{cases} S\ L\ \mathbf{H}_t^{\alpha_1}\ \mathcal{T} = \Lambda\ I_{N+1} - (\tau+\mu)\ S\ L\ \mathcal{T} - \beta\ S\ L\ \Phi(E,L)\ \mathcal{T}, \\ E\ L\ \mathbf{H}_t^{\alpha_2}\ \mathcal{T} = \beta\ S\ L\ \Phi(E,L)\ \mathcal{T} - (\gamma+\mu+\eta+\sigma)\ E\ L\ \mathcal{T}, \\ Q\ L\ \mathbf{H}_t^{\alpha_3}\ \mathcal{T} = \tau\ S\ L\ \mathcal{T} + \gamma\ E\ L\ \mathcal{T} - (\mu+\upsilon+\theta)\ Q\ L\ \mathcal{T}, \\ A\ L\ \mathbf{H}_t^{\alpha_4}\ \mathcal{T} = \sigma\ E\ L\ \mathcal{T} + \theta\ Q\ L\ \mathcal{T} - (\mu+\zeta_1)\ A\ L\ \mathcal{T}, \\ M\ L\ \mathbf{H}_t^{\alpha_5}\ \mathcal{T} = \eta\ E\ L\ \mathcal{T} + \upsilon\ Q\ L\ \mathcal{T} - (\mu+\delta+\zeta_2)\ M\ L\ \mathcal{T}, \\ R\ L\ \mathbf{H}_t^{\alpha_6}\ \mathcal{T} = \zeta_1\ A\ L\ \mathcal{T} + \zeta_2\ M\ L\ \mathcal{T} - \mu\ R\ L\ \mathcal{T}. \end{cases} \tag{4.3}$$

Applying the Tau method, unknown vectors are computed by using the orthogonal property of shifted Legendre polynomials on Ω. Hence, by utilizing the definition of inner product (2.6), we will have:

$$\begin{aligned}\big\langle \mathbf{H}_t^{\alpha_i}\ \mathcal{T}, \mathcal{L}_w(t)\big\rangle &= \Big[\big\langle (\mathbf{H}_t^{\alpha_i}\ \mathcal{T})_j, \mathcal{L}_w(t)\big\rangle\Big]_{j=1}^{N}\\ &= \Big[\frac{\Re(\alpha_i)\Gamma(j+1)}{1-\alpha_i}\ \sum_{k=0}^{\infty}\Big(\frac{-\alpha_i}{1-\alpha_i}\Big)^k \frac{1}{\Gamma(j+1+\alpha_i k)} \times \int_{\Omega} t^{j+\alpha_i k}\mathcal{L}_w(t)\ dt\ \Big]_{j=1}^{N}\\ &= \Big[(\mathbf{H}^{\alpha_i})_j\Big]_{j=1}^{N} = \mathbf{H}^{\alpha_i},\ \ i=1,2,...,6,\ \ w=0,1,...,N,\end{aligned}$$

and $(\mathbf{H}^{\alpha_i})_0 = 0$. Additionally, we assume that the infinite series of the Mittag-Leffler function is considered up to 20 term in numerical examples. In view of the exactness of Legendre Gauss quadrature for all polynomials with a maximum degree of $2N+1$, we have:

$$\begin{aligned}\big\langle \mathcal{T}, \mathcal{L}_w(t)\big\rangle &= \int_{\Omega} \mathcal{T}\mathcal{L}_w(t)\ dt = \Big[\int_{\Omega} t^j \mathcal{L}_w(t)\ dt\Big]_{j=0}^{N}\\ &= \Big[\big\langle t^j, \mathcal{L}_w(t)\big\rangle_N\Big]_{j=0}^{N} = \overline{\mathcal{T}}.\end{aligned}$$

Thereby, projecting (4.3) on $\{\mathcal{L}_w(t)\}_{w=0}^{N}$ and using the above relations yield:

$$\begin{cases} S\ L\ \mathbf{H}^{\alpha_1} = \Lambda - (\tau+\mu)\ S\ L\ \overline{\mathcal{T}} - \beta\ S\ L\ \Phi(E,L)\ \overline{\mathcal{T}},\\ E\ L\ \mathbf{H}^{\alpha_2} = \beta\ S\ L\ \Phi(E,L)\ \overline{\mathcal{T}} - (\gamma+\mu+\eta+\sigma)\ E\ L\ \overline{\mathcal{T}},\\ Q\ L\ \mathbf{H}^{\alpha_3} = \tau\ S\ L\ \overline{\mathcal{T}} + \gamma\ E\ L\ \overline{\mathcal{T}} - (\mu+\upsilon+\theta)\ Q\ L\ \overline{\mathcal{T}},\\ A\ L\ \mathbf{H}^{\alpha_4} = \sigma\ E\ L\ \overline{\mathcal{T}} + \theta\ Q\ L\ \overline{\mathcal{T}} - (\mu+\zeta_1)\ A\ L\ \overline{\mathcal{T}},\\ M\ L\ \mathbf{H}^{\alpha_5} = \eta\ E\ L\ \overline{\mathcal{T}} + \upsilon\ Q\ L\ \overline{\mathcal{T}} - (\mu+\delta+\zeta_2)\ M\ L\ \overline{\mathcal{T}},\\ R\ L\ \mathbf{H}^{\alpha_6} = \zeta_1\ A\ L\ \overline{\mathcal{T}} + \zeta_2\ M\ L\ \overline{\mathcal{T}} - \mu\ R\ L\ \overline{\mathcal{T}}.\end{cases} \tag{4.4}$$

Now, we have a $(6N+6)\times(6N+6)$ system of nonlinear algebraic equations in which the unknown vectors and consequently the discrete approximations $\mathbb{S}_N$, $\mathbb{E}_N$, $\mathbb{Q}_N$, $\mathbb{I}_{sN}$, $\mathbb{I}_{aN}$ and $\mathbb{R}_N$ can be determined by imposing the initial conditions:

$$S\ L\ e_1 = \mathbb{S}_0,\qquad E\ L\ e_1 = \mathbb{E}_0,\qquad Q\ L\ e_1 = \mathbb{Q}_0,$$

$$A\ L\ e_1 = \mathbb{I}_{a0},\qquad M\ L\ e_1 = \mathbb{I}_{s0},\qquad R\ L\ e_1 = \mathbb{R}_0,$$

where $e_1 = [1,0,0,...,0]^T$ is a column vector of order $N+1$. For this purpose, we replace the first column of each of the system equations (4.4) with one of the boundary conditions, respectively.

Now, a natural question is to investigate whether the obtained solutions in this section are convergent to the exact solutions of such a system of fractional differential equations or not. This issue will be discussed in the next section.

5. Convergence Analysis

In this section, we consider the convergence of described approach in section 4 by making the error bounds of the approximate solutions in L^2 norm. The next theorem presents suitable bounds for the error functions of Tau approximations of system (3.1).

Theorem 5.1. *Suppose that the following conditions are exist:*

- $\mathbb{S}(t) \in \mathcal{S}^{m_1}(\Omega)$, $\mathbb{E}(t) \in \mathcal{S}^{m_2}(\Omega)$, $\mathbb{Q}(t) \in \mathcal{S}^{m_3}(\Omega)$,
- $\mathbb{I}_a(t) \in \mathcal{S}^{m_4}(\Omega)$, $\mathbb{I}_s(t) \in \mathcal{S}^{m_5}(\Omega)$, $\mathbb{R}(t) \in \mathcal{S}^{m_6}(\Omega)$,

for $m_1, m_2, ..., m_6 \geq 0$. Moreover, let relations given by (4.1) be the Tau approximations of (3.1). Then, for sufficiently large N, we have:

$$
\begin{aligned}
\left\|e_{\mathbb{S}}(t)\right\| &\leq C_1 N^{-m_1}\left|{}^{\mathcal{ABC}}\mathcal{D}_t^{\alpha_1}(\mathbb{S})\right|_{m_1} + C_2 N^{-m_2}\left|{}^{\mathcal{ABC}}\mathcal{D}_t^{\alpha_2}(\mathbb{E})\right|_{m_2},\\
\left\|e_{\mathbb{E}}(t)\right\| &\leq C_3 N^{-m_1}\left|{}^{\mathcal{ABC}}\mathcal{D}_t^{\alpha_1}(\mathbb{S})\right|_{m_1} + C_4 N^{-m_2}\left|{}^{\mathcal{ABC}}\mathcal{D}_t^{\alpha_2}(\mathbb{E})\right|_{m_2},\\
\left\|e_{\mathbb{Q}}(t)\right\| &\leq C_5 N^{-m_1}\left|{}^{\mathcal{ABC}}\mathcal{D}_t^{\alpha_1}(\mathbb{S})\right|_{m_1} + C_6 N^{-m_2}\left|{}^{\mathcal{ABC}}\mathcal{D}_t^{\alpha_2}(\mathbb{E})\right|_{m_2} + C_7 N^{-m_3}\left|{}^{\mathcal{ABC}}\mathcal{D}_t^{\alpha_3}(\mathbb{Q})\right|_{m_3},\\
\left\|e_{\mathbb{I}_a}(t)\right\| &\leq C_8 N^{-m_1}\left|{}^{\mathcal{ABC}}\mathcal{D}_t^{\alpha_1}(\mathbb{S})\right|_{m_1} + C_9 N^{-m_2}\left|{}^{\mathcal{ABC}}\mathcal{D}_t^{\alpha_2}(\mathbb{E})\right|_{m_2}\\
&\quad + C_{10} N^{-m_3}\left|{}^{\mathcal{ABC}}\mathcal{D}_t^{\alpha_3}(\mathbb{Q})\right|_{m_3} + C_{11} N^{-m_4}\left|{}^{\mathcal{ABC}}\mathcal{D}_t^{\alpha_4}(\mathbb{I}_a)\right|_{m_4},\\
\left\|e_{\mathbb{I}_s}(t)\right\| &\leq C_{12} N^{-m_1}\left|{}^{\mathcal{ABC}}\mathcal{D}_t^{\alpha_1}(\mathbb{S})\right|_{m_1} + C_{13} N^{-m_2}\left|{}^{\mathcal{ABC}}\mathcal{D}_t^{\alpha_2}(\mathbb{E})\right|_{m_2}\\
&\quad + C_{14} N^{-m_3}\left|{}^{\mathcal{ABC}}\mathcal{D}_t^{\alpha_3}(\mathbb{Q})\right|_{m_3} + C_{15} N^{-m_5}\left|{}^{\mathcal{ABC}}\mathcal{D}_t^{\alpha_4}(\mathbb{I}_s)\right|_{m_5},\\
\left\|e_{\mathbb{R}}(t)\right\| &\leq C_{16} N^{-m_1}\left|{}^{\mathcal{ABC}}\mathcal{D}_t^{\alpha_1}(\mathbb{S})\right|_{m_1} + C_{17} N^{-m_2}\left|{}^{\mathcal{ABC}}\mathcal{D}_t^{\alpha_2}(\mathbb{E})\right|_{m_2}\\
&\quad + C_{18} N^{-m_3}\left|{}^{\mathcal{ABC}}\mathcal{D}_t^{\alpha_3}(\mathbb{Q})\right|_{m_3} + C_{19} N^{-m_4}\left|{}^{\mathcal{ABC}}\mathcal{D}_t^{\alpha_4}(\mathbb{I}_a)\right|_{m_4}\\
&\quad + C_{20} N^{-m_5}\left|{}^{\mathcal{ABC}}\mathcal{D}_t^{\alpha_5}(\mathbb{I}_s)\right|_{m_5} + C_{21} N^{-m_6}\left|{}^{\mathcal{ABC}}\mathcal{D}_t^{\alpha_6}(\mathbb{R})\right|_{m_6},
\end{aligned} \tag{5.1}
$$

where $e_\vartheta(t) = \vartheta(t) - \vartheta_N(t)$ is the error function and C_i s are constants which do not depend on N.

Proof. According to the described strategy in previous section, the Tau approximations (4.1) satisfy in the following system:

$$
\begin{cases}
\mathcal{P}_N\left({}^{\mathcal{ABC}}\mathcal{D}_t^{\alpha_1}\mathbb{S}_N(t)\right) = \Lambda - (\tau+\mu)\ \mathbb{S}_N(t) - \beta\ \mathbb{S}_N(t)\ \mathbb{E}_N(t),\\
\mathcal{P}_N\left({}^{\mathcal{ABC}}\mathcal{D}_t^{\alpha_2}\mathbb{E}_N(t)\right) = \beta\ \mathbb{S}_N(t)\ \mathbb{E}_N(t) - (\gamma+\mu+\eta+\sigma)\ \mathbb{E}_N(t),\\
\mathcal{P}_N\left({}^{\mathcal{ABC}}\mathcal{D}_t^{\alpha_3}\mathbb{Q}_N(t)\right) = \tau\ \mathbb{S}_N(t) + \gamma\ \mathbb{E}_N(t) - (\mu+\upsilon+\theta)\ \mathbb{Q}_N(t),\\
\mathcal{P}_N\left({}^{\mathcal{ABC}}\mathcal{D}_t^{\alpha_4}\mathbb{I}_{aN}(t)\right) = \sigma\ \mathbb{E}_N(t) + \theta\ \mathbb{Q}_N(t) - (\mu+\zeta_1)\ \mathbb{I}_{aN}(t),\\
\mathcal{P}_N\left({}^{\mathcal{ABC}}\mathcal{D}_t^{\alpha_5}\mathbb{I}_{sN}(t)\right) = \eta\ \mathbb{E}_N(t) + \upsilon\ \mathbb{Q}_N(t) - (\mu+\delta+\zeta_2)\ \mathbb{I}_{sN}(t),\\
\mathcal{P}_N\left({}^{\mathcal{ABC}}\mathcal{D}_t^{\alpha_6}\mathbb{R}_N(t)\right) = \zeta_1\ \mathbb{I}_{aN}(t) + \zeta_2\ \mathbb{I}_{sN}(t) - \mu\ \mathbb{R}_N(t).
\end{cases} \tag{5.2}
$$

Subtracting (5.2) from (3.1) together with some simple computations, we will have:

$$
\begin{cases}
{}^{\mathcal{ABC}}\mathcal{D}_t^{\alpha_1}e_{\mathbb{S}}(t) = -(\tau+\mu)\ e_{\mathbb{S}}(t) - \beta\ \mathbb{E}(t)\ e_{\mathbb{S}}(t) - \beta\ \mathbb{S}_N(t)\ e_{\mathbb{E}}(t) + \ e_{\mathcal{P}_N}\left({}^{\mathcal{ABC}}\mathcal{D}_t^{\alpha_1}\mathbb{S}_N\right),\\
{}^{\mathcal{ABC}}\mathcal{D}_t^{\alpha_2}e_{\mathbb{E}}(t) = \beta\ \mathbb{E}(t)\ e_{\mathbb{S}}(t) + \beta\ \mathbb{S}_N(t)\ e_{\mathbb{E}}(t) - (\gamma+\mu+\eta+\sigma)\ e_{\mathbb{E}}(t) + \ e_{\mathcal{P}_N}\left({}^{\mathcal{ABC}}\mathcal{D}_t^{\alpha_2}\mathbb{E}_N\right),\\
{}^{\mathcal{ABC}}\mathcal{D}_t^{\alpha_3}e_{\mathbb{Q}}(t) = \tau\ e_{\mathbb{S}}(t) + \gamma\ e_{\mathbb{E}}(t) - (\mu+\upsilon+\theta)\ e_{\mathbb{Q}}(t) + e_{\mathcal{P}_N}\left({}^{\mathcal{ABC}}\mathcal{D}_t^{\alpha_3}\mathbb{Q}_N\right),\\
{}^{\mathcal{ABC}}\mathcal{D}_t^{\alpha_4}e_{\mathbb{I}_a}(t) = \sigma\ e_{\mathbb{E}}(t) + \theta\ e_{\mathbb{Q}}(t) - (\mu+\zeta_1)\ e_{\mathbb{I}_a}(t) + e_{\mathcal{P}_N}\left({}^{\mathcal{ABC}}\mathcal{D}_t^{\alpha_4}\mathbb{I}_{aN}\right),\\
{}^{\mathcal{ABC}}\mathcal{D}_t^{\alpha_5}e_{\mathbb{I}_s}(t) = \eta\ e_{\mathbb{E}}(t) + \upsilon\ e_{\mathbb{Q}}(t) - (\mu+\delta+\zeta_2)\ e_{\mathbb{I}_s}(t) + e_{\mathcal{P}_N}\left({}^{\mathcal{ABC}}\mathcal{D}_t^{\alpha_5}\mathbb{I}_{sN}\right),\\
{}^{\mathcal{ABC}}\mathcal{D}_t^{\alpha_6}e_{\mathbb{R}}(t) = \zeta_1\ e_{\mathbb{I}_a}(t) + \zeta_2\ e_{\mathbb{I}_s}(t) - \mu\ e_{\mathbb{R}}(t) + e_{\mathcal{P}_N}\left({}^{\mathcal{ABC}}\mathcal{D}_t^{\alpha_6}\mathbb{R}_N\right),
\end{cases} \tag{5.3}
$$

where $e_{\mathcal{P}_N}(\vartheta) = \vartheta - \mathcal{P}_N(\vartheta)$. By applying the fractional integral operator ${}^{\mathcal{ABC}}\mathcal{I}_t^{\alpha_1}$ on both sides of the first equation (5.3) and using the first relation in (2.4), we conclude that:

$$
e_{\mathbb{S}}(t) = -(\tau+\mu)\ {}^{\mathcal{ABC}}\mathcal{I}_t^{\alpha_1}(e_{\mathbb{S}}(t)) - \beta\ {}^{\mathcal{ABC}}\mathcal{I}_t^{\alpha_1}(\mathbb{E}(t)\ e_{\mathbb{S}}(t)) - \beta\ {}^{\mathcal{ABC}}\mathcal{I}_t^{\alpha_1}(\mathbb{S}_N(t)\ e_{\mathbb{E}}(t)) + {}^{\mathcal{ABC}}\mathcal{I}_t^{\alpha_1}\Big(e_{\mathcal{P}_N}\left({}^{\mathcal{ABC}}\mathcal{D}_t^{\alpha_1}\mathbb{S}_N\right)\Big). \tag{5.4}
$$

Due to the definition of Riemann-Liouville integral operator (2.1) and using (2.3) in (5.4), we get:

$$\begin{aligned} e_{\mathbb{S}}(t) =& \frac{-(\tau+\mu)\ (1-\alpha_1)}{\Re(\alpha_1)} e_{\mathbb{S}}(t) - \frac{\alpha_1(\tau+\mu)}{\Re(\alpha_1)}\ {}^{R}I_t^{\alpha_1}(e_{\mathbb{S}}(t)) - \frac{\beta(1-\alpha_1)}{\Re(\alpha_1)}\mathbb{E}(t)e_{\mathbb{S}}(t) - \frac{\beta\ \alpha_1}{\Re(\alpha_1)}\ {}^{R}I_t^{\alpha_1}(\mathbb{E}(t)\ e_{\mathbb{S}}(t)) \\ &- \frac{\beta(1-\alpha_1)}{\Re(\alpha_1)}\mathbb{S}_N(t)\ e_{\mathbb{E}}(t) - \frac{\beta\ \alpha_1}{\Re(\alpha_1)}\ {}^{R}I_t^{\alpha_1}(\mathbb{S}_N(t)\ e_{\mathbb{E}}(t)) + \frac{1-\alpha_1}{\Re(\alpha_1)} e_{\mathcal{P}_N}\left({}^{\mathcal{ABC}}\mathcal{D}_t^{\alpha_1}\mathbb{S}_N\right) \\ &+ \frac{\alpha_1}{\Re(\alpha_1)}\ {}^{R}I_t^{\alpha_1}\Big(e_{\mathcal{P}_N}\left({}^{\mathcal{ABC}}\mathcal{D}_t^{\alpha_1}\mathbb{S}_N\right)\Big). \end{aligned} \tag{5.5}$$

Now, by taking a 2−norm of both sides of (5.5) and applying the boundedness property of Riemann-Liouville integral, i.e., Lemma 2.5, we achieve:

$$\big\|e_{\mathbb{S}}(t)\big\| \le d_{11}\big\|e_{\mathbb{S}}(t)\big\| + d_{12}\big\|e_{\mathbb{E}}(t)\big\| + \left|\frac{1}{\Re(\alpha_1)}\right|\ \Big\|e_{\mathcal{P}_N}\left({}^{\mathcal{ABC}}\mathcal{D}_t^{\alpha_1}\mathbb{S}_N\right)\Big\|, \tag{5.6}$$

where

$$\begin{aligned} d_{11} &= \left|\frac{\tau+\mu}{\Re(\alpha_1)}\right| + \left|\frac{\beta}{\Re(\alpha_1)}\right| \max_{t\in\Omega}\|\mathbb{E}(t)\|, \\ d_{12} &= \left|\frac{\beta}{\Re(\alpha_1)}\right| \max_{t\in\Omega}\|\mathbb{S}_N(t)\|, \end{aligned}$$

and similarly, for the second equation of (5.3), it follows that:

$$\big\|e_{\mathbb{E}}(t)\big\| \le d_{21}\big\|e_{\mathbb{S}}(t)\big\| + d_{22}\big\|e_{\mathbb{E}}(t)\big\| + \left|\frac{1}{\Re(\alpha_2)}\right|\ \Big\|e_{\mathcal{P}_N}\left({}^{\mathcal{ABC}}\mathcal{D}_t^{\alpha_2}\mathbb{E}_N\right)\Big\|,$$

such that:

$$\begin{aligned} d_{21} &= \left|\frac{\beta}{\Re(\alpha_2)}\right| \max_{t\in\Omega}\|\mathbb{E}(t)\|, \\ d_{22} &= \left|\frac{\beta}{\Re(\alpha_2)}\right| \max_{t\in\Omega}\|\mathbb{S}_N(t)\| + \left|\frac{\gamma+\mu+\eta+\sigma}{\Re(\alpha_2)}\right|, \end{aligned}$$

and consequently:

$$\big\|e_{\mathbb{E}}(t)\big\| \le \frac{d_{21}}{1-d_{22}}\big\|e_{\mathbb{S}}(t)\big\| + \left|\frac{1}{(1-d_{22})\Re(\alpha_2)}\right|\ \Big\|e_{\mathcal{P}_N}\left({}^{\mathcal{ABC}}\mathcal{D}_t^{\alpha_2}\mathbb{E}_N\right)\Big\|. \tag{5.7}$$

Substituting (5.7) into (5.6) and assuming $u = \left|1 - d_{11} - \frac{d_{12}d_{21}}{1-d_{22}}\right| \neq 0$ gives:

$$\big\|e_{\mathbb{S}}(t)\big\| \le K_1\Big\|e_{\mathcal{P}_N}\left({}^{\mathcal{ABC}}\mathcal{D}_t^{\alpha_1}\mathbb{S}_N\right)\Big\| + K_2\Big\|e_{\mathcal{P}_N}\left({}^{\mathcal{ABC}}\mathcal{D}_t^{\alpha_2}\mathbb{E}_N\right)\Big\|, \tag{5.8}$$

where

$$K_1 = \frac{1}{|\Re(\alpha_1)|\ u}, \qquad K_2 = \left|\frac{d_{12}}{\Re(\alpha_2)(1-d_{22})u}\right|.$$

According to the hypotheses of this theorem and definition of ABC-derivatives (2.2), we can see, obviously

$${}^{\mathcal{ABC}}\mathcal{D}_t^{\alpha_1}\mathbb{S}_N(t) = \frac{\Re(\alpha_1)}{1-\alpha_1}\sum_{j=0}^{\infty}\left(\frac{-\alpha_1}{1-\alpha_1}\right)^j \frac{1}{\Gamma(\alpha_1 j+1)}\int_0^t \mathbb{S}'_N(x)(t-x)^{\alpha_1 j}dx \in \mathcal{S}^{m_1}(\Omega), \tag{5.9}$$

and similarly ${}^{\mathcal{ABC}}\mathcal{D}_t^{\alpha_2}\mathbb{E}_N(t) \in \mathcal{S}^{m_2}(\Omega)$. Therefore, by using Lemma 2.4, one can imply:

$$\begin{aligned} \Big\|e_{\mathcal{P}_N}\left({}^{\mathcal{ABC}}\mathcal{D}_t^{\alpha_1}\mathbb{S}_N\right)\Big\| &\le C\ N^{-m_1}\left|{}^{\mathcal{ABC}}\mathcal{D}_t^{\alpha_1}\mathbb{S}_N\right|_{m_1} \\ &\le CN^{-m_1}\Big(\left|{}^{\mathcal{ABC}}\mathcal{D}_t^{\alpha_1}\mathbb{S}\right|_{m_1} + \left|{}^{\mathcal{ABC}}\mathcal{D}_t^{\alpha_1}e_{\mathbb{S}}\right|_{m_1}\Big), \\ \Big\|e_{\mathcal{P}_N}\left({}^{\mathcal{ABC}}\mathcal{D}_t^{\alpha_2}\mathbb{E}_N\right)\Big\| &\le CN^{-m_2}\Big(\left|{}^{\mathcal{ABC}}\mathcal{D}_t^{\alpha_2}\mathbb{E}\right|_{m_2} + \left|{}^{\mathcal{ABC}}\mathcal{D}_t^{\alpha_2}e_{\mathbb{E}}\right|_{m_2}\Big), \end{aligned} \tag{5.10}$$

and thereby, inserting relations (5.10) into (5.8) and ignoring some unnecessary terms for sufficiently large values of N, the desired error estimation (5.1) for $\mathbb{S}(t)$ can be obtained. Also, replacing the error boundary of $\mathbb{S}(t)$ and property (5.9) into (5.7) leads to the favorable result of error estimation (5.1) for $\mathbb{E}(t)$. In the same way, by applying the fractional integral operator ${}^{\mathcal{ABC}}\mathcal{I}_t^{\alpha_3}$ on both sides of the third equation (5.3), we conclude that:

$$\big\|e_{\mathbb{Q}}(t)\big\| \leq \tau\big\|e_{\mathbb{S}}(t)\big\| + \gamma\big\|e_{\mathbb{E}}(t)\big\| + \left|\frac{\mu+\upsilon+\theta}{\Re(\alpha_3)}\right| \big\|e_{\mathbb{Q}}(t)\big\| + \left|\frac{1}{\Re(\alpha_3)}\right| \left\|e_{\mathcal{P}_N}\left({}^{\mathcal{ABC}}\mathcal{D}_t^{\alpha_3}\mathbb{Q}_N\right)\right\|,$$

so that by assumptions $1-\left|\frac{\mu+\upsilon+\theta}{\Re(\alpha_3)}\right| \neq 0$ and $\mathbb{Q}(t) \in \mathcal{S}^{m_3}(\Omega)$ and inserting obtained error boundaries of functions $\mathbb{S}(t)$ and $\mathbb{E}(t)$, the following inequality holds:

$$\big\|e_{\mathbb{Q}}(t)\big\| \leq C_5\ N^{-m_1}\big|{}^{\mathcal{ABC}}\mathcal{D}_t^{\alpha_1}(\mathbb{S})\big|_{m_1} + C_6\ N^{-m_2}\big|{}^{\mathcal{ABC}}\mathcal{D}_t^{\alpha_2}(\mathbb{E})\big|_{m_2} + C_7\ N^{-m_3}\big|{}^{\mathcal{ABC}}\mathcal{D}_t^{\alpha_3}(\mathbb{Q})\big|_{m_3}.$$

Finally, in order to find the error boundary of functions $\mathbb{I}_a(t)$, $\mathbb{I}_s(t)$ and $\mathbb{R}(t)$, it is enough to take ABC-integrals ${}^{\mathcal{ABC}}\mathcal{I}_t^{\alpha_4}$, ${}^{\mathcal{ABC}}\mathcal{I}_t^{\alpha_5}$ and ${}^{\mathcal{ABC}}\mathcal{I}_t^{\alpha_6}$ from the sides of the last three equations (5.3), respectively. Then, proceeding in the same manner, based on the appropriate assumptions and the previous obtained estimations, the boundaries (5.1) are derived. □

Since that the rate of convergence is exponential, the analysis presented above clearly demonstrates that the proposed Tau approximations for the system of fractional differential equations of various orders, (3.1), produce a highly accurate numerical solution.

6. Numerical Examples

To illustrate the effectiveness of the mathematical analysis of the ABC-derivative COVID-19 model (3.1), some numerical examples are presented using the proposed Tau method. Before implementing Tau method for model (3.1), we give a simple test problem to explain the power of the described approach for solving a system of fractional differential equations with multi-order. To demonstrate the effectiveness of our presented technique, we compare our scheme to the numerical scheme given forward by [3, 22]. Note that all the calculations were supported by Mathematica® software.

Example 6.1. Consider the following system of multi-order fractional differential equation

$$\begin{cases} {}^{\mathcal{ABC}}\mathcal{D}_t^{0.5}x(t) = x(t) - y(t) + \varphi_1(t), \\ {}^{\mathcal{ABC}}\mathcal{D}_t^{0.3}y(t) = 2x(t) + y(t) + \varphi_2(t), \end{cases} \qquad t \in [0,1], \tag{6.1}$$

where the functions $\varphi_1(t)$ and $\varphi_2(t)$ are obtained such that the exact solutions are $x(t) = y(t) = t^2$. In first, we implement the the described Legendre Tau method for the numerical solution of (6.1). Suppose that:

$$x_N(t) = \sum_{i=0}^{N} x_i\mathcal{L}_i(t), \qquad y_N(t) = \sum_{i=0}^{N} y_i\mathcal{L}_i(t),$$

as the approximate solutions of (6.1) that are obtained by using the proposed method in the section 4.

To compare our method with the other approaches and to show the efficiency of our proposed method, we apply the recent numerical scheme proposed in the references [3, 22]. For this task, using the Atangana-Baleanu fractional integral operator (2.3) on both sides of the equations (6.1) and applying the two points Lagrange interpolation polynomial for

TABLE 2. The numerical errors of the our proposed method with different values of N for Example 6.1.

N	$e(x)$	$e(y)$	$CPU\ time$
2	2.5376×10^{-4}	6.5752×10^{-4}	20.607
4	2.6538×10^{-5}	6.9767×10^{-5}	48.298
6	5.6572×10^{-6}	1.5560×10^{-5}	89.858
8	1.7324×10^{-6}	5.0320×10^{-6}	148.232
10	6.6964×10^{-7}	2.0383×10^{-6}	232.522
12	8.0949×10^{-8}	2.5809×10^{-7}	331.044

TABLE 3. The numerical errors of the proposed method in [3, 22] with different values of N for Example 6.1.

N	$\tilde{e}(x)$	$\tilde{e}(y)$	$CPU\ time$
2	5.3465×10^{-1}	8.5971×10^{-1}	15.460
4	1.3529×10^{-2}	6.8774×10^{-2}	45.287
6	4.2679×10^{-3}	5.5291×10^{-3}	100.839
8	4.6131×10^{-4}	5.9876×10^{-4}	168.324
10	2.3458×10^{-4}	3.8459×10^{-4}	272.003
12	1.3589×10^{-5}	2.0058×10^{-4}	425.071

the simplification of the obtained integrals, we will have for $k = 0, 1, 2, ...$

$$\begin{aligned} x(t_{k+1}) &= x(t_0) + \frac{0.5(x(t_k) - y(t_k) + \varphi_1(t_k))}{\Re(0.5)} + \frac{0.5}{\Re(0.5)} \times \sum_{m=0}^{k} \Big[\frac{h^{0.5}(x(t_m) - y(t_m) + \varphi_1(t_m))}{\Gamma(2.5)} \big[(k+1-m)^{0.5} \\ &\times (k-m+2.5) - (k-m)^{0.5}(k-m+3)\big] - \frac{h^{0.5}(x(t_{m-1}) - y(t_{m-1}) + \varphi_1(t_{m-1}))}{\Gamma(2.5)} \\ &\times \big[(k+1-m)^{1.5} - (k-m)^{0.5}(k-m+1.5)\big]\Big], \\ y(t_{k+1}) &= y(t_0) + \frac{0.7(2x(t_k) + y(t_k) + \varphi_2(t_k))}{\Re(0.3)} + \frac{0.7}{\Re(0.3)} \times \sum_{m=0}^{k} \Big[\frac{h^{0.3}(2x(t_m) + y(t_m) + \varphi_2(t_m))}{\Gamma(2.3)} \big[(k+1-m)^{0.3} \\ &\times (k-m+2.3) - (k-m)^{0.3}(k-m+2.6)\big] - \frac{h^{0.3}(2x(t_{m-1}) + y(t_{m-1}) + \varphi_2(t_{m-1}))}{\Gamma(2.3)} \\ &\times \big[(k+1-m)^{1.3} - (k-m)^{0.3}(k-m+1.3)\big]\Big], \end{aligned}$$

therefore, we obtain the approximate solutions $\tilde{x}_N(t) = x(t_N)$ and $\tilde{y}_N(t) = y(t_N)$ for different values $N = k+1$ of the above system. We assume that the error functions for these methods are calculated by:

$$e(x) = \|x(t) - x_N(t)\|, \qquad e(y) = \|y(t) - y_N(t)\|,$$
$$\tilde{e}(x) = \|x(t) - \tilde{x}_N(t)\|, \qquad \tilde{e}(y) = \|y(t) - \tilde{y}_N(t)\|.$$

Then, the results for different values of the approximation degree N are reported in Table 2, Table 3 and Figure 1. Comparing the reported results approves the superiority and reliability of the our proposed scheme over the presented method in [3, 22].

In overall, Figure 1 confirms that the spectral accuracy is achieved for the Tau method, because the logarithmic representation of errors has almost linear behavior versus N as well as predicted by Theorem 5.1. In addition, the used CPU time based on second, for the different values of N, is listed in Table 2 and Table 3.

Now, we are ready to implement Tau method to the mathematical model of COVID-19.

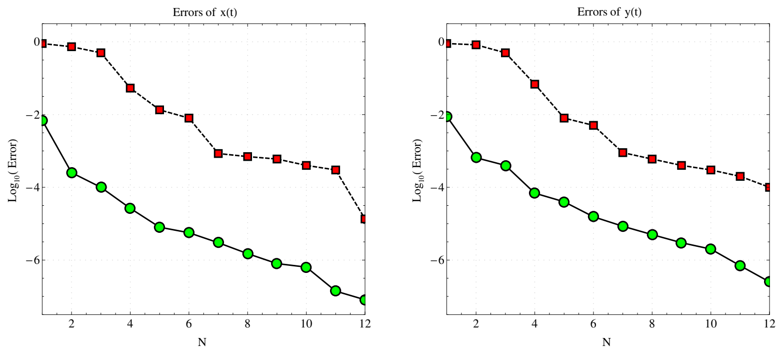

FIGURE 1. Comparison of the obtained errors between our method (solid lines) and the method of [3, 22] (dashed lines) with different values of N for Example 6.1.

TABLE 4. Values of the parameters used in model (3.1).

Parameter	value
τ	0.002
β	0.0805
δ	1.6728×10^{-5}
γ	2.0138×10^{-4}
η	0.4478
σ	0.0668
θ	0.0101
ζ_1	5.734×10^{-5}
ζ_2	1.6728×10^{-5}
Λ	0.02537
μ	0.0106

Example 6.2. Consider the system of multi-order fractional differential equations (3.1) for the COVID-19 disease model with the approximate solutions (4.1) for $N = 4$. To generate the simulation results for this system, the biological parameters determined from the real data presented in reference [3] which are supplied in Table 4 are used. Also, the initial conditions for the model variables are $\mathbb{S}(0) = 0.5$, $\mathbb{E}(0) = 0.2$, $\mathbb{Q}(0) = 0.1$, $\mathbb{I}_a(0) = 0.1$, $\mathbb{I}_s(0) = 0.1$, $\mathbb{R}(0) = 0$ in [3] and days are used as the measure of time.

First, assuming $t \in [0, 30]$, we simulate the COVID-19 model (3.1) for various values of fractional orders α_i for all of the state variables. The results are plotted in Figure 2. These representations show that the approximate solutions of the system of fractional differential equations (3.1) tend to the exact solutions as α_i tends to 1. This demonstrates the effectiveness and dependability of the Tau method for approximating practical models. As we can see, increasing the fractional order of the parameters causes the population of a community to become more infected. It should be noted that the other orders are considered to be constant and equal to 0.5 when one of the orders α_i tends to one.

Figure 2 show the effect of fractional exponent on the behavior of the populations $\mathbb{S}$, $\mathbb{E}$, $\mathbb{Q}$, $\mathbb{I}_a$, $\mathbb{I}_s$, and $\mathbb{R}$ over time. COVID-19 spread through social contact, contact with infected individuals, and contact with infected surfaces. As can be seen, the population of those who have been exposed, infected, quarantined, recovered, or removed grows exponentially over time. According to Figure 2, the number of susceptible people will exhibit fluctuating behavior over time since they may end up in an exposed or infected class. Data from global statistics up to the present can be used to see these patterns because the number of infected persons is increasing along with this exponential behavior.

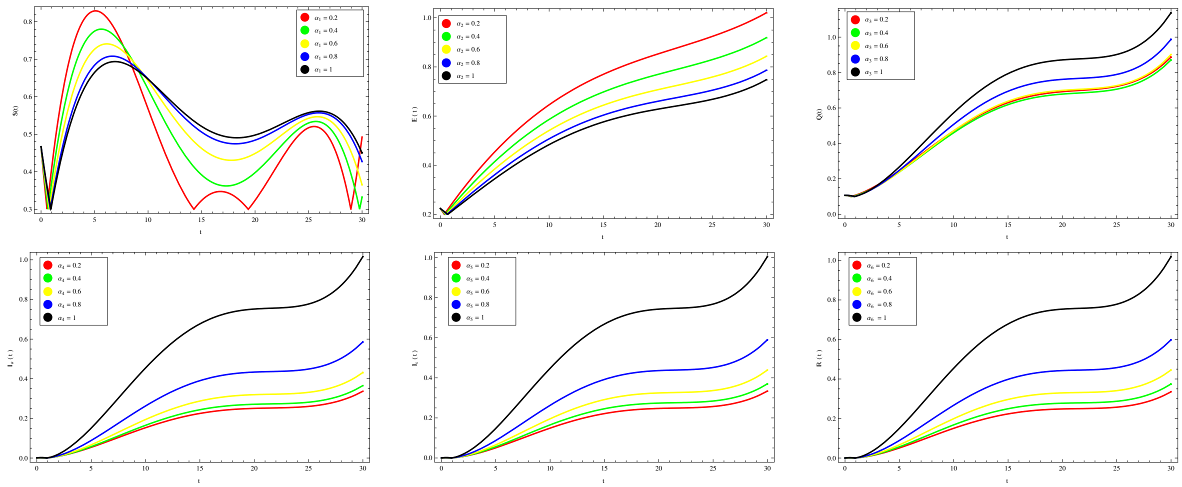

FIGURE 2. Graphical representation for behavior of each state variable with different fractional order for $N = 4$.

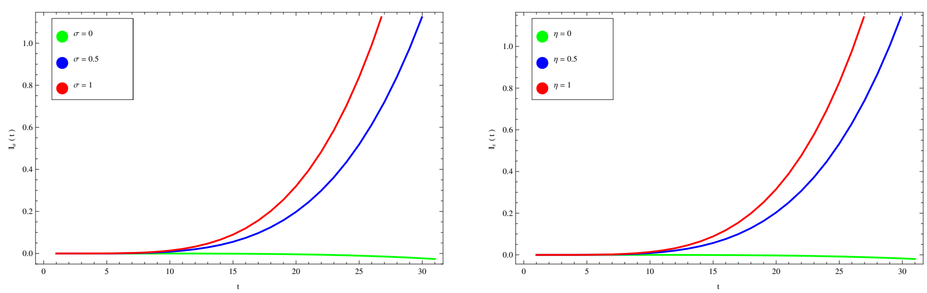

FIGURE 3. Behavior of $\mathbb{I}_s(t)$ and $\mathbb{I}_a(t)$ with different transfer rates for $N = 4$.

These findings concur with those reported in the references [22, 23]. As a result, it is clear that the proposed method in this paper is effective and appropriate.

In the following step, we simulate model (3.1) by increasing the transfer rate of persons from exposed class to symptomatic and asymptomatic infective individuals in order to investigate the impact of the contact rate on COVID-19 disease. In contrast, we use the Tau method with $N = 4$ to approximate the solutions to (3.1) at various rates of η and σ. The results are graphed in Figure 3. This figure shows that, as we predicted, when the transfer rate increases, the number of symptomatic and asymptotically infected people increases. On the other hand, increasing the transmission rate causes more people to become infected in less time. As shown in Figure 3, the number of symptomatic and asymptomatic infected people does not change over time when the transfer rates η and σ are zero.

7. Conclusion

In this article, we presented a spectral Tau method to simulate the numerical results of the COVID-19 pandemic which is modeled by using factors like the number of susceptible, exposed, asymptotically and symptomatic infected, quarantined, recovered individuals and transfer rates between them in the form of fractional differential equations with ABC-derivatives. We were able to construct a form of operational matrix for fractional differentiation with the Mittag-Leffler kernel. This paper's most important achievement is that we can exponentially explain the errors of Tau approximations, which is a desired property for spectral approaches. Then, the accuracy of the suggested Tau approach in this study is demonstrated by an illustrative example. Additionally, we depicted and discussed the simulation results for various values of fractional orders in the mathematical model of COVID-19 disease, which indicated the coronavirus influence on different variables over time. Also, the effect of increased transfer rates between exposed and infected individuals is examined, and the results show a significant impact, with the result that the number of infected people increases as transfer rates rise. These numerical results can be applied to manage the infection. Future studies using fractional models can identify how COVID-19 epidemics are influenced by vaccination and other controlling factors.

Declarations

Conflict of interest On behalf of all authors, the corresponding author states that there is no conflict of interest.

References

[1] M. A. Aba Oud, A. Ali, H. Alrabaiah, S. Ullah, M. A. Khan, and S. Islam, *A fractional order mathematical model for COVID-19 dynamics with quarantine, isolation, and environmental viral load*, Adv. Differ. Equ., *106* (2021), 1–12.

[2] T. Abdeljawad and D. Baleanu, *Integration by parts and its applications of a new nonlocal fractional derivative with Mittag-Leffler nonsingular kernel*, J. Nonlinear Sci. Appl., *10* (2017), 1098–1107.

[3] I. Ahmed, G. U. Modu, A. Yusuf, P. Kumam, and I. Yusuf, *A mathematical model of Coronavirus Disease (COVID-19) containing asymptomatic and symptomatic classes*, Results. Phys., *21* (2021), 103776.

[4] B. S. T. Alkahtani, *Chuás circuit model with Atangana-Baleanu derivative with fractional order*, Chaos. Solitons. Fractals, *89* (2016), 547–551.

[5] E. S. Allman and J. A. Rhodes, *Mathematical models in biology: An Introduction*, Cambridge University Press, 2003.

[6] R. M. Anderson and R. M. May, *Helminth infections of humans: mathematical models, population dynamics, and control*, Adv. Parasitol., *24* (1985), 1–101.

[7] A. A. M, Arafa, I. M. Hanafy, and M. I. Gouda, *Stability analysis of fractional order HIV infection of* $+T$ *cells with numerical solutions*, J. Fract. Calc. Appl., *7* (2016), 36–45.

[8] A. Atangana, *On the new fractional derivative and application to nonlinear Fisher reaction-diffusion equation*, Appl. Math. Comput., *273* (2016), 948–956.

[9] A. Atangana and D. Baleanu, *New fractional derivatives with nonlocal and non-singular kernel: Theory and application to heat transfer model*, Therm. Sci., *20* (2016), 763–769.

[10] F. Brauer and C. Castillo-Chávez, *Mathematical Models in Population Biology and Epidemiology*, Texts Appl. Math., 2001.

[11] C. Canuto, M. Y. Hussaini, A. Quarteroni, and T. A. Zang, *Spectral Methods, Fundamentals in Single Domains*, Springer-Verlag, Berlin, 2006.

[12] K. Diethelm, *The Analysis of Fractional Differential Equations*, Berlin Heidelberg, Springer-Verlag, 2010.

[13] K. Diethelm, N. J. Ford, A. D. Freed, and Y. U. Luchko, *Algorithmsfor thefractional calculus selection of numerical methods*, Comput. Methods. Appl. Mech. Eng., *194* (2005), 743–773.

[14] X. L. Ding and Y. L. Jiang, *Waveform relaxation method for fractional differential algebraic equations*, Fract. Calc. Appl. Anal., *17* (2014), 585–604.

[15] J. Djordjevic, C. J. Silva, and D. F. M. Torres, *A stochastic SICA epidemic model for HIV transmission*, Appl. Math. Lett., *84* (2018), 168–175.

[16] L. Edelstein-Keshet, *Mathematical models in biology*, SIAM, 2005.

[17] F. Ghanbari, K. Ghanbari, and P. Mokhtary, *Generalized Jacobi-Galerkin method for nonlinear fractional differential algebraic equations*, Comp. Appl. Math., *37* (2018), 5456–5475.

[18] F. Ghanbari, K. Ghanbari, and P. Mokhtary, *High-order Legendre collocation method for fractional-order linear semi-explicit differential algebraic equations*, Electron. Trans. Numer. Anal., *48* (2018), 387–406.

[19] F. Ghoreishi and M. Hadizadeh, *Numerical computation of the Tau approximation for the Volterra-Hammerstein integral equations*, Numer. Algor., *52* (2009), 541–559.

[20] J. F. Gómez, L. Torres, and R. F. Escobar, *Fractional Derivatives with Mittag-Leffler Kernel*, Springer, 2019.

[21] J. Hesthaven, S. Gottlieb, and D. Gottlieb, *Spectral Methods for Time-Dependent Problems*, Cambridge University Press, Cambridge, 2007.
[22] M. A. Khan and A. Atangana, *Modeling the dynamics of novel coronavirus (2019-nCov) with fractional derivative*, Alex. Eng. J., *59* (2020), 2379–2389.
[23] S. Kumar, J. Cao, and M. Abdel-Aty, *A novel mathematical approach of COVID-19 with non-singular fractional derivative*, Chaos Solit. Fractals, *139* (2020), 110048.
[24] B. P. Moghaddam, J. A. T. Machado, and A. Babaei, *A computationally efficient method for tempered fractional differential equations with application*, Appl. Math. Comput., *37* (2018), 3657–3671.
[25] F. Ndaïrou, I. Area, J. J. Nieto, and D. F. M. Torres, *Mathematical modeling of COVID-19 transmission dynamics with a case study of Wuhan*, Chaos Solit. Fractals, *135* (2020), 109846.
[26] F. Ndaïrou, I. Area, J. J. Nieto, C. J. Silva, and D. F. M. Torres, *Mathematical modeling of Zika disease in pregnant women and newborns with microcephaly in Brazil*, Math. Methods. Appl. Sci., *41* (2018), 8929–8941.
[27] K. Parand, H. Yousefi, M. Fotouhifar, M. Delkhosh, and M. Hosseinzadeh, *Shifted Boubaker Lagrangian approach for solving biological systems*, Int. J. Biomath., *11* (2018).
[28] K. Parand, Z. Kalantari, and M. Delkhosh, *Quasilinearization-Lagrangian method to solve the HIV infection model of CD4(Math Processing Error) T cells*, SeMA. J., *75* (2018), 271-283.
[29] K. Parand, F. Mirahmadian, and M. Delkhosh, *The pseudospectral Legendre method for solving the HIV infection model of CD4+T cells*, Nonlinear Studies, *25* (2018), 241–250.
[30] I. Podlubny, *Fractional Differential Equations*, New York, Academic Press, 1999.
[31] A. Rachah and D. F. M. Torres, *Dynamics and optimal control of Ebola transmission*, Math. Comput. Sci., *10* (2016), 331–342.
[32] P. Rahimkhani and Y. Ordokhani, *The bivariate Müntz wavelets composite collocation method for solving space-time fractional partial differential equations*, Comput. Appl. Math., *39* (2020), 3–29.
[33] P. Rahimkhani and Y. Ordokhani, *Approximate solution of nonlinear fractional integro-differential equations using fractional alternative Legendre functions*, J. Comput. Appl. Math., *365* (2020), 112365.
[34] P. Rahimkhani and Y. Ordokhani, *Numerical solution a class of 2D fractional optimal control problems by using 2D Muntz-Legendre wavelets*, Optimal Control Appl. Methods, *39* (2018), 1916–1934.
[35] P. Rahimkhani and Y. Ordokhani, *A numerical scheme based on Bernoulli wavelets and collocation method for solving fractional partial differential equations with Dirichlet boundary conditions*, Numer. Method Partial Differential Equation, *35* (2018), 6–21.
[36] P. Riyapan, S. E. Shuaib, and A. Intarasit, *A Mathematical Model of COVID-19 Pandemic: A Case Study of Bangkok, Thailand*, Comput. Math. Methods Med., *2021* (2021), 11 pages.
[37] J. Shen, T. Tang, and L. L. Wang, *Spectral Methods Algorithms, Analysis and Applications*, Springer-Verlag, Berlin, 2011.
[38] S. Wang, W. Tang, L. Xiong, M. Fang, B. Zhang, C. Y. Chiu, and R. Fan, *Mathematical modeling of transmission dynamics of COVID-19*, Big Data. Inf. Anal., *6* (2021), 12–25.
[39] D. Yan and H. Cao, *The global dynamics for an age-structured tuberculosis transmission model with the exponential progression rate*, Appl. Math. Model., *75* (2019), 769–786.